Artificial Neural Networks Approach to Fractional Snow Cover Mapping

ILIYANA D. DOBERVA1 AND ANDREW G. KLEIN [2]

ABSTRACT

Binary snow maps represent pixels as simply snow-covered or snow-free and their accuracy is dependent on the spatial resolution of the remotely-sensed images used in creating them. Fractional snow cover (FSC) mapping overcomes the problem of low spatial resolution of images by assigning estimated snow fraction to each pixel. There are two commonly used methods for estimating FSC from Moderate Resolution Imaging Spectroradiometer (MODIS). One is linear spectral un-mixing while the other employs the empirical relationship between Normalized Difference Snow Index (NDSI) and snow fraction. Machine learning is an alternative to these methods for estimating FSC. Advantages of Artificial Neural Networks (ANNs) are that they can easily incorporate auxiliary information such as land cover type and are capable of learning non-linear relationships. This study trains a feed-forward neural network with backpropagation to estimate FSC from MODIS surface reflectance, Normalized Difference Snow Index (NDSI), Normalized Difference Vegetation Index (NDVI) and land cover. Independent estimates of FSC for training and validation are created from Landsat Enhanced Thematic Mapper Plus (ETM+) binary snow cover maps. The developed ANN compares favorably to the standard MODIS FSC product. However, it overestimates FSC at low FSC and underestimates it at high FSC. The average Root Mean Square (RMS) error of the ANN FSC for three independent Landsat ETM+ scenes is 11.93%.

Keywords: snow fraction, snow cover, neural networks, MODIS

INTRODUCTION

Snow cover extent is a parameter in both hydrologic and climate models (Rango, 1996; Roesch *et at.*, 2001) and it is also monitored to supply information for climate change studies (Lemke *et al.*, 2007). Snow cover information can be collected *in situ*. However, *in situ* methods remain problematic for measuring snow cover extent as the site where snow is sampled may not be representative of the entire study area, and the sampled site only gives snow cover state at a particular location and does not provide information about whether the surrounding terrain is also snow-covered (Bales *et al.*, 2006). Adverse weather conditions in snow-covered areas and the remoteness of these areas often make manual collection of consistent snow cover information physically impossible (Derksen and LeDrew, 2000).

[1] Department of Geography, MS 3147, Texas A&M University, College Station, TX 77853-3147, email: iliyanad@neo.tamu.edu
[2] Department of Geography, MS 3147, Texas A&M University, College Station, TX 77853-3147, email: klein@geog.tamu.edu

Spaceborne and airborne remote sensing offers an alternative to *in situ* collection of snow cover extent measurements. Using satellite remote sensing for monitoring snow cover is advantageous because it offers consistent data collection over a large area. In this respect, long-term studies and environmental models have a continuous supply of snow cover measurements (König *et al.*, 2001).

Traditional snow cover maps are binary which means that pixels are mapped as either snow-covered or snow-free. The current standard algorithm for producing global daily snow maps from Moderate Resolution Imaging Spectroradiometer (MODIS) maps snow primarily using Normalized Difference Snow Index (NDSI) as a threshold; a Normalized Difference Vegetation Index (NDVI) threshold is, also, used to improve snow detection in forests (Hall *et al.*, 1995, 2002; Klein *et al.*, 1998).

Fractional Snow Cover Mapping

Fractional snow cover (FSC) mapping overcomes the limitations of low spatial resolution of daily images such as those provided by MODIS by representing snow cover in each pixel as a percentage of the area of the pixel. Since a pixel integrates the spectral information of the whole area viewed, the snowpack cannot be spatially located within the pixel. However, it is possible to estimate the percentage of snow in a pixel. This is an improvement over traditional binary snow cover maps which represent a pixel simply as either snow-covered or snow-free. Typically in binary snow maps, a pixel is classified as containing snow if approximately fifty percent of its area is snow-covered (Hall *et al.*, 2002). This may introduce significant error in the estimations of the spatial extent of snow cover, which in return may cause erroneous results in hydrological (Rango, 1996) and General Circulation Models (GCMs) (Roesch *et al.*, 2001). Even slight variations in FSC produce significantly different results in GCMs and consequently, incorrect estimates of FSC result in biased climate predictions (Niu and Yang, 2007).

A pixel contains the spectral information from all surface components within a sensor's Instantaneous Field Of View (IFOV). Linear mixture analysis is performed with the assumption that the spectral information within a pixel is a linear combination of the surface components within that pixel and that the weight of each component equals the proportion of the pixel's IFOV that contains the component (Jensen, 2005). Endmembers are idealized, pure spectral signatures for a type of surface (Schowengerdt, 1997). The performance of the spectral un-mixing model depends on availability of complete and accurate endmembers which are usually stored in a spectral library referenced by the model during processing.

Linear spectral unmixing has been widely applied in snow fraction mapping (Nolin *et al.*, 1993; Simpson *et al.*, 1998; Shi, 1999; Simpson and McIntire, 2001; Vikhamer and Solberg, 2002, 2003; Painter *et al.*, 2003, 2009; Romanov *et al.*, 2003; Foppa *et al.*; 2004, Hongen and Suhong, 2004; Metsämäki *et al.*, 2005). These applications require an extensive endmember library for success. Methods differ on how endmembers are collected and how the mapping algorithm determines which endmembers should be included in un-mixing each pixel to determine FSC.

Establishing an empirical relationship between satellite reflectance and FSC to determine FSC is another approach. A method developed for the Terra and Aqua MODIS instruments (Salomonson and Appel, 2004, 2006) uses Normalized Difference Snow Index (NSDI) constructed from MODIS bands 4 and 7, which record reflectance in the green and short-wave infrared ranges of the spectrum, respectively. A statistical linear relationship between NDSI and snow fraction in a MODIS pixel is established by using higher resolution Landsat snow maps as an estimate of true snow fraction. This method is currently used to create the standard MODIS FSC snow cover product.

Artificial Neural Networks (ANNs) are a machine learning technique which can learn relationships between specified input and output variables. Neural networks constitute an information processing model that stores empirical knowledge through a learning process and subsequently makes the stored knowledge available for future use (Haykin, 1999). Often the learning process in ANNs is called training. Various remote sensing applications have utilized ANNs for subpixel estimation of a number of surfaces types (Foody *et al.*, 1997; Tatem *et al.*, 2002; Shabanov *et al.*, 2005; Lee and Lathrop, 2006). Advantages of neural networks are that there is no need to assume a linear relationship between surface components in a pixel, end-members are not necessary, and auxiliary information such as land cover is easily incorporated.

Study purpose and objectives

This study investigated if ANNs were applicable to successful mapping of snow fraction. To accomplish this aim, a neural network was trained and tested on fifteen Landsat Enhanced Thematic Mapper Plus (ETM+) training areas within North America representative of the different land covers typical of the snow-covered portions of the Northern Hemisphere. Inputs to the network were the seven 500-m MODIS land surface reflectance bands provided in the Surface Reflectance Daily L2G Global 1km and 500m (MOD09GA) product (Vermonte and Kotchenova, 2008), NDSI and NDVI which were calculated from the reflectance bands, and land cover in the International Geosphere-Biosphere Programme (IGBP) classification scheme from the MODIS/ Terra Land Cover 96 Day L3 Global 1 km ISIN Grid (MOD12Q1) product (Hodges, 2009) (Table 1). A reference snow fraction was determined by applying the SNOMAP (Hall *et al.*, 1995) algorithm to higher resolution Landsat ETM+ images. The neural network was trained on eleven Landsat snow maps representative of different land covers and tested on three additional Landsat snow maps.

Table 1: Input to the ANN

MOD09GA Band 1	Reflectance at 620-670 nm
MOD09GA Band 2	Reflectance at 841-876 nm
MOD09GA Band 3	Reflectance at 459-479 nm
MOD09GA Band 4	Reflectance at 545-565 nm
MOD09GA Band 5	Reflectance at 1230-1250 nm
MOD09GA Band 6	Reflectance at 1628-1652 nm
MOD09GA Band 7	Reflectance at 2105-2155 nm
NDSI	(Band4–Band6)/(Band4+Band6)
NDVI	(Band2–Band1)/(Band2+Band1)
MOD12Q1	IGBP Land cover Classification

METHODOLOGY

This study used a feed-forward neural network trained in a supervised manner through backpropagation. During backpropagation training, the network was initialized with random weights and learning involved adjusting the weights so that the error between the generated output and the supplied ‘true’ or target output was minimized.

The performance of ANNs trained in a supervised manner was closely related to the quality of the data set used for training (Priddy and Keller, 2005), and therefore a training data set should be representative of the pixels that it would be used on. In the current study, it was important that the training examples were not biased towards any land cover but instead adequately represented the land covers typical of mid- and high-latitude environments. The training set should also not be biased towards particular snow cover fractions.

Landsat Scene Selection and Preprocessing

Selection of training and test scenes was restricted to partially snow-covered images acquired within North America during different months of the year. The main objective in selecting the training scenes was to represent land covers typical of the snow-covered mid to high latitudes. The land cover classification system used in selecting samples combined the seventeen IGBP land cover classes into eight: evergreen forest, deciduous forest, mixed forest, mixed agriculture, barren/sparsely vegetated, tundra, grasslands/shrublands and wetlands (Table 2). A similar approach was used previously by Hall *et al.* (2001) to assess the accuracy of the MODIS snow product. These eights classes were subsequently combined into three to assess the accuracy of the ANN FSC algorithm.

Table 2. Land cover classes used in the study

<table>
<tr><th>IGBP Land Cover Classes</th><th>Reclassified For Sampling</th><th>Reclassified For Testing</th></tr>
<tr><td>Evergreen needleleaf forest</td><td rowspan="2">Evergreen Forests</td><td rowspan="5">Forest 1</td></tr>
<tr><td>Evergreen broadleaf forest</td></tr>
<tr><td>Deciduous needleleaf forest</td><td rowspan="2">Deciduous Forests</td></tr>
<tr><td>Deciduous broadleaf forest</td></tr>
<tr><td>Mixed forests</td><td>Mixed Forests</td></tr>
<tr><td>Croplands</td><td rowspan="3">Mixed agriculture</td><td rowspan="3">Mixed agriculture 2</td></tr>
<tr><td>Urban and built-up</td></tr>
<tr><td>Cropland/natural vegetation mosaic</td></tr>
<tr><td>Barren/sparsely vegetated</td><td>Barren/sparsely vegetated</td><td rowspan="7">Non forest 3</td></tr>
<tr><td>Woody savannas</td><td rowspan="2">Tundra</td></tr>
<tr><td>Savannas</td></tr>
<tr><td>Closed shrublands</td><td rowspan="3">Grasslands/shrublands</td></tr>
<tr><td>Open shrublands</td></tr>
<tr><td>Grasslands</td></tr>
<tr><td>Permanent wetlands</td><td>Wetlands</td></tr>
<tr><td>Permanent snow and ice</td><td>n/a</td><td>n/a</td></tr>
<tr><td>Water</td><td>n/a</td><td>n/a</td></tr>
</table>

The Landsat ETM+ scenes were selected for minimal cloud cover and were acquired between 2000 when MODIS became operational and 2003 when the Landsat ETM+ Scan Line Corrector (*SLC*) failed degrading image quality (National Aeronautics and Space Administration, 2009). Three of the selected scenes were previously used in developing the NDSI snow fraction method for mapping FSC (Salomonson and Appel 2004, 2006).

Landsat ETM+ images were obtained free of charge at a Level 1T processing from the United States Geological Survey (USGS) Earth Resources Observation and Science (EROS) data center. This product was corrected from distortions related to sensor, satellite and Earth effects. All scenes were georegistered to a UTM projection with a WGS84 datum.

Each of the Landsat ETM+ images was converted to radiance using a standard approach (National Aeronautics and Space Administration, 2009). Atmospheric correction and conversion to radiance was then performed using the Fast Line-of-sight Atmospheric Analysis of Spectral Hypercubes (FLAASH) module in ENVI 4.5 software package (Kaufmann, *et al.*, 1997). For three of the scenes (Table 3), FLAASH was unsuccessful and therefore a modified black body correction (Chavez, 1988) was applied.

Finally, the atmospherically corrected scenes were compared to orthorectified Landsat images which were acquired through the Global Land Cover Facility (Global Land Cover Facility, 2009). Most of the scenes (Table 3) had to be georegistered through selection of Ground Control Points (GCPs) because of geolocation differences between the orthorectified scenes and the ones used in the study. At least fifteen GCPs were selected for each scene with a Root Mean Square (RMS) error of less than 0.1 pixels.

Landsat Snow Maps

Each of the pre-processed Landsat ETM+ images was used as input to the snow cover mapping algorithm SNOMAP (Hall *et al*, 1995) which classified pixels as either snow-covered or snow-free. SNOMAP is the snow mapping algorithm used in the standard MODIS snow cover product and has a long heritage in snow mapping. The 30-m Landsat snow maps were then used to calculate snow fraction within each MODIS pixel. The land surface reflectance bands provided in

MOD09GA have a 500 m spatial resolution. However, errors with MODIS geolocation (Wolfe, 2007) mean that each pixel had sampled a slightly larger area. A common approach in resampling snow fraction to MODIS pixel size is to calculate the fraction within a large circle around a pixel (Painter *et al.*, 2009). In this study, resampling was performed within a 750-meter-radius circle around each MODIS pixel which means that the analyzed spatial footprint was 1.77 km^2.

Table 3. Landsat ETM+ Training (1 through 11) and Test (A, B and C) Scenes

Scene	WRS-2 Path/Row	Date Acquired	Predominant Reclassified-For-Sampling Land Covers	Number of Samples
1[1, 2]	24/23	04/24/2000	Tundra, grasslands/shrublands, wetlands	4,400
2	24/28	12/10/2002	Deciduous forests, mixed forests, mixed agriculture	6,209
3	24/28	02/28/2003	Deciduous forests, mixed forests	1,853
4	26/29	02/07/2002	Deciduous forests, mixed forests, mixed agriculture	2,446
5	26/30	02/07/2002	Mixed agriculture	1,288
6	38/21	12/25/2001	Evergreen forests	1,400
7	38/22	03/19/2003	Evergreen forests, mixed forests, tundra	2,228
8	39/22	11/01/2002	Evergreen forests, mixed forests, mixed agriculture, tundra	4,625
9	39/24	11/01/2002	Mixed agriculture, grasslands/shrublands	2,000
10[1, 2, 3]	65/17	05/12/2001	Tundra, grasslands/shrublands	3,400
11[1, 2, 3]	73/11	05/23/2002	Barren/sparsely vegetated, grasslands/shrublands	1,800
A[2, 3]	11/20	11/07/2000	Barren/sparsely vegetated, grasslands/shrublands	61,531
B	43/21	04/19/2002	Evergreen forests, mixed forests	116,874
C	25/28	04/08/2003	Deciduous forests, mixed forests, mixed agriculture	96,282

[1] Modified Black Body Atmospheric correction used instead of FLAASH.
[2] Additional georeferencing was not performed
[3] Scene used in developing MODIS FSC product (Salomonson and Appel 2004, 2006)

MODIS Processing

Water was excluded from the analysis using the water mask acquired from the MODIS land cover product MOD12Q1. Areas identified by visual examination as cloud covered in the Landsat images were also masked. Finally, the cloud state and quality data sets provided with the MOD09GA product were analyzed to exclude pixels that were cloud-covered, mixed, fell within cloud shadow or had been produced at less than ideal quality.

Sampling

A total of eleven Landsat snow maps (Figure 1) were sampled to create training, validation and test data sets. Following usage in the ANNs literature both the training and validation data sets were used during network training. The samples from the training data set were used in adjusting the weights of the ANN. After each training iteration, the validation data set was used to measure the generalization performance of the network as represented by the mean square error (MSE) between the ANN FSC output and reference FSC output. Training ended when MSE began to increase indicating overtraining of the network (Haykin, 1999).

Sample points were selected using stratified random sampling. Stratification was done by land cover (eight classes) and by snow cover fraction which was categorized in 0.1 intervals to create ten FSC classes. After sampling, the eleven Landsat ETM+ images used for creating the reference snow maps were visually examined and it was determined that some clouds had not been detected before sample points were selected. Therefore, 297 points were removed from the sample data set because of apparent contamination by cloud cover or shadows. The final sample data set included 31,649 observations. It was then split in three fractions. One half of the samples were used for training, a fourth of the samples for network validation and the remaining for testing the trained network.

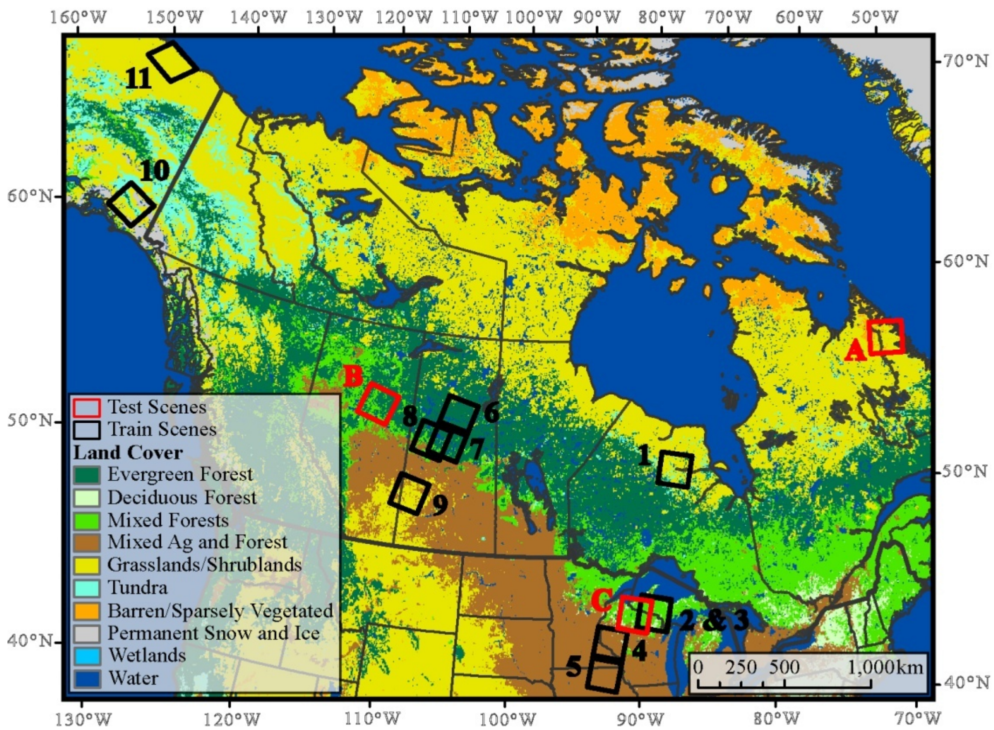

Figure 1. Training and test sites are located in North America. Training sites are selected representative of various land covers.

Three additional Landsat snow maps (Figure 1) were selected and reserved to independently test the results on scenes not used during training. Test Scene A (Table 3) was located in Labrador, Canada and contained barren/sparsely vegetated and grassland/shrublands land covers. Test Scene B contained evergreen and mixed forests and was located in Alberta, Canada. And Test Scene C contained deciduous and mixed forests and mixed agriculture. It was located in Michigan and Wisconsin, United States. All of the available MODIS pixels covering these scenes were used.

Network Inputs

Nine inputs were provided to the ANN (Table 1). Seven MODIS surface reflectance bands were provided in the MOD09GA product. Calculated NDSI and NDVI were used to emphasize snow covered areas and vegetated areas, respectively. Land cover in the IGBP classification scheme was used as an input because spectral characteristics could vary across land covers. Even though training samples were selected from eight combined classes the complete IGBP classification system was used as input to the ANN so that the network could learn to differentiate between slightly different classes such as evergreen needleleaf forest and evergreen broadleaf forest.

ANN Configuration

Feed-forward ANN implementation in the Neural Network Toolbox in MATLAB R2008b was used in this study. Important network configurations were summarized in Table 4. One hidden layer was chosen as it had been demonstrated that a single hidden layer can learn any mapping (Priddy and Keller, 2005). The number of hidden layer neurons was chosen to be 20, twice the number of inputs, after experimenting with 10 and 30 hidden layer neurons networks produced similar results.

The neural network generated some snow fraction values above 1 and below 0. In FSC mapping such values are unrealistic as a pixel cannot have a negative amount of snow cover and cannot have snow cover exceeding 100 percent of the pixel. Therefore, FSC values larger than 1 were set to 1 and smaller than 0 were set to 0.

Some of the network parameters were determined by testing the performance of the network while holding initial weights constant during the different runs. Performance of the network was determined by examining the RMS error of the test data set and the three independent Landsat test scenes and by visually comparing the resulting ANN FSC maps to the reference FSC maps.

A tangent hyperbolic transfer function between the input and hidden layer was selected for the final network but a logistic sigmoid transfer function was also tested. Both of these transfer functions are sigmoid functions which is the most common transfer function in ANNs (Haykin, 1999). The ANN normalization method applied scaled each input feature between -1 and 1. Several other common normalization methods were also tested including: scaling between 0.1 and 0.9 for the tangent hyperbolic transfer function, scaling between 0 and 1 and between 0.1 and 0.9 for the logistic sigmoid transfer function, and mapping each feature’s mean to 0 and its standard deviation to 1. Overall these normalization schemes produced FSC maps of similar quality.

Table 4. Neural Network Description and Parameters

Training method	Levenberg-Marquardt backpropagation (supervised)
Learning method	Gradient descent with momentum weight and bias learning function
Performance measure	Mean Square Error (MSE)
Network architecture	Nine input neurons, one hidden layer with 20 hidden layer neurons, and one output neuron
Transfer functions	Tangent hyperbolic between input and hidden layers; Linear between hidden and output layers
Input/output normalization	Each input band is scaled between -1 and 1

After configuring the network, the sample data set which included the pixels randomly sampled from the eleven Landsat training scenes was examined. Approximately 200 samples had errors of computed FSC larger than three standard deviations of the mean and were removed. The network was trained on the remaining data set. Different runs were performed allowing for random initialization of weights. The ANN initialized with the saved initial weights had best performance and its results were further analyzed by examining scatter plots comparing the neural network generated FSC and reference FSC for each of the Landsat reference training scenes. The estimated FSC of the samples from training scene 3 (Table 3) was considerably underestimated. Samples from this scene were removed and a final ANN was trained using the saved initial weights.

RESULTS AND DISCUSSION

Overall, the ANN approach appears to do an adequate job of mapping FSC. Agreement between the Landsat reference FSC and the ANN-estimated FSC was good with the Coefficient of

Determination (R^2) ranging from 0.80 to 0.91 (Table 5). This was also illustrated through scatterplots of reference Landsat FSC versus ANN FSC (Figure 2). While, overall agreement was high, the neural network appeared to overestimate snow fraction at low FSC and underestimate it at high FSC.

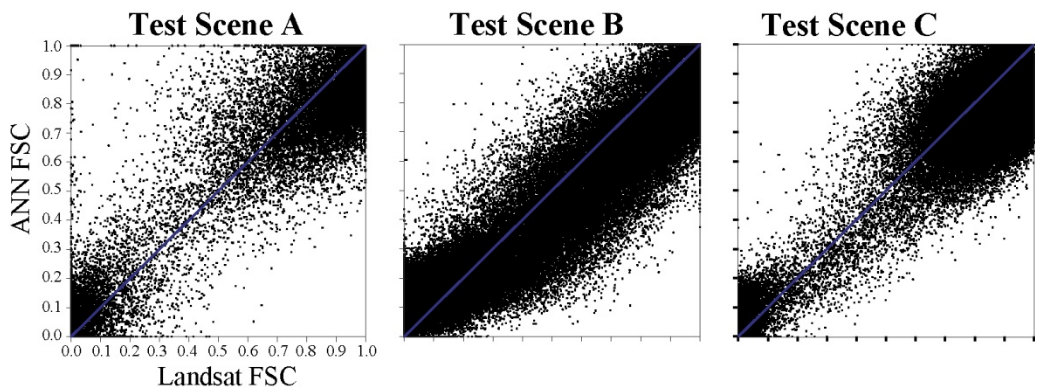

Figure 2. Scatter plot graphs showing ANN FSC results and Landsat snow map FSC for the three test scenes. The blue line is the 1:1 line.

The underestimation of FSC is also evident by comparing Landsat and ANN snow fraction maps (Figures 3, 4 and 5). The darker colors on the ANN snow fraction map of the Labrador test scene (Figure 3) indicate lower FSC than the lighter colors for the same areas showing high FSC on the reference snow fraction map. The ANN FSC map of the test scene over Saskatchewan (Figure 4) had lower FSC than the reference FSC map. However, the ANN FSC captures the spatial variability of snow cover with the same areas having most and least snow fraction in both ANN and reference FSC maps. Spatial variability of ANN FSC was least in the test scene over Michigan and Wisconsin.

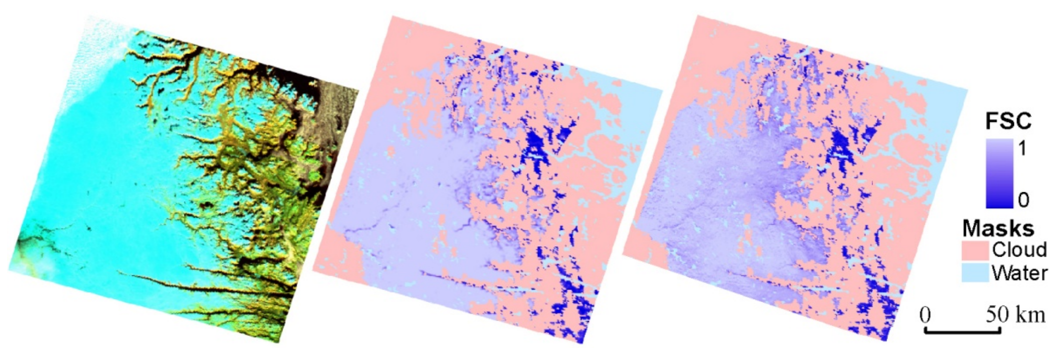

Figure 3. ANN results of the network over Test Scene A are displayed. A false-color image composite of MODIS bands 6, 2 and 1 as R, G and B shows snow as cyan colors (a). Reference snow map shows pixels covered with large snow fraction as light blue and snow-free pixels as dark blue (b). Neural network FSC map is displayed (c).

Table 5 summarizes errors between ANN and Landsat FSC maps. Not surprisingly, RMS error between ANN FSC and reference FSC (10.39%) was lowest over the non forested Labrador test scene. The two forested scenes had slightly higher but similar RMS errors of 12.66% for Saskatchewan and 12.75% for Michigan. The three test scenes' RMS errors were also analyzed for the three combined land cover categories (Table 6). The RMS error over mixed agriculture was largest at 13.85%, followed by forest at 12.54% and no forest at 10.79%.

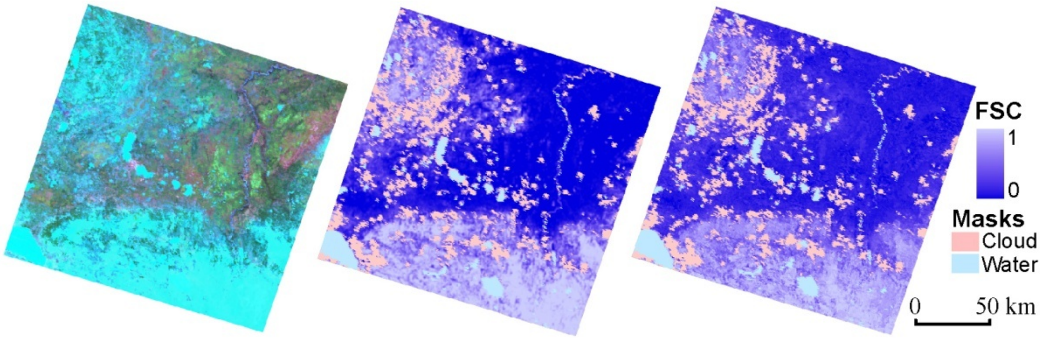

Figure 4. The results of the network over Test Scene B. The displayed maps are patterned after those in Figure 3

The ANN FSC was also compared to the FSC provided as part of the MODIS/Terra Snow Cover Daily L3 Global 500m Grid (MOD10A1) product (Riggs *et al.*, 2006) (Tables 4 and 5). With exception of the Labrador test scene the ANN RMS errors were comparable to the MOD10A1 FSC. The better fit of MOD10A1 FSC for the Labrador test scene may be because thise scene was used in the development of the MODIS snow fraction algorithm. Based on the two test scenes not used in the developing of the MODIS FSC method, the ANN and the empirical NDSI approaches achieve similar FSC accuracy when compared to the reference Landsat snow maps.

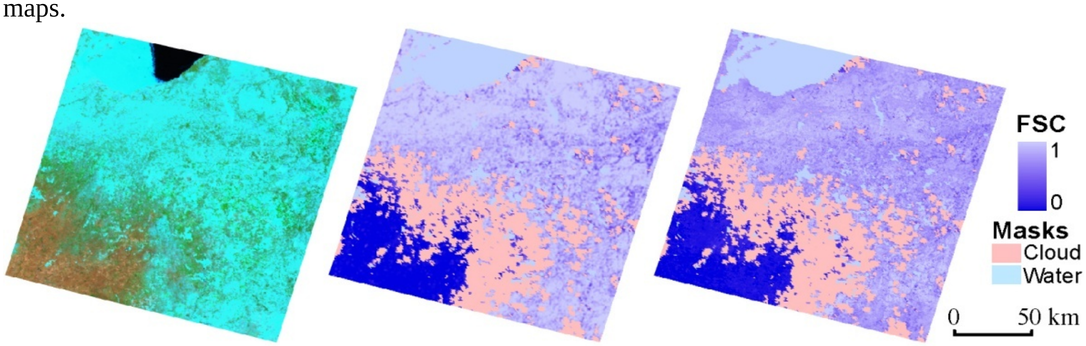

Figure 5. The results of the network over Test Scene C are displayed. The displayed maps are patterned after those in Figure 3

Table 5. RMSE and R^2 between ANN FSC and reference FSC and between MOD10 FSC and reference FSC

	Test Samples		**Test Scene A**		**Test Scene B**		**Test Scene C**	
	R^2	RMSE	R^2	RMSE	R^2	RMSE	R^2	RMSE
ANN	0.80	13.30%	0.89	10.39%	0.89	12.66%	0.91	12.75%
MOD10A1	n/a	n/a	0.91	8.99%	0.90	12.16%	0.89	12.50%

Table 6. RMSE and R2 per combined land cover category

	Forests		**Mixed Agriculture**		**No Forest**	
Number of samples	192, 418		15,817		66, 452	
	R^2	RMSE	R^2	RMSE	R^2	RMSE
ANN	0.92	12.54%	0.97	13.85%	0.90	10.79%
MOD10A1	0.91	12.61%	0.97	7.46%	0.92	9.37%

Vikamar and Solbergs (2003) reported R^2 of 0.95 and 0.85 for observed and modeled through linear spectral unmixing snow fraction over the forested parts of their study area. These also compared well with the ANN FSC as the R^2 of the three independent test scenes was between 0.89 and 0.91. The most recent study of linear mixture analysis for FSC mapping (Painter *et al.*, 2009), reported an average RMS error of 5% for snow-covered pixels. The validation scenes in this study were located in parts of the Colorado Rocky Mountains, the Sierra Nevada of California, the headwaters of the Rio Grande, and the Himalayas where the characteristics were varying topography and vegetation. For example, no vegetation, brush, meadows and alpine tundra were present in the high altitudes while coniferous and desciduous forests were present at the lower elevations of the validation areas.

CONCLUSIONS AND FUTURE WORK

In this study, a neural network trained with backpropagation successfully learned the relationship between MODIS snow fraction and surface reflectance in seven wavelength bands, NDSI, NDVI and land cover. The network was applied to scenes independent of those used for training and results were compared to reference Landsat snow maps and to the MODIS FSC product. The ANN performance across the test scenes and across different land cover types was comparable to the standard MODIS snow fraction product.

This was the first study that the authors were aware of training a neural network to estimate snow cover fraction. The network architecture employed was a very traditional backpropagation feed-forward network. Improved snow mapping accuracy may be obtained by developing a more sophisticated ANN or through additional inputs such as tree cover fraction, elevation or through possibly including MODIS thermal bands in the network.

REFERENCES

Bales RC, Molotch NP, Painter TH, Dettinger MD, Rice R, Dozier J. 2006. Mountain hydrology of the western United States. *Water Resources Research* **42**. DOI: 10.1029/2005WR004387.

Chavez PS. 1988. An improved dark-object subtraction technique for atmospheric scattering correction of multispectral data. *Remote Sensing of Environment* **24**: 459-479.

Derksen C, LeDrew E. 2000. Variability and change in terrestrial snow cover: data acquisition and links to the atmosphere. *Progress in Physical Geography* **24**: 469-498.

Foody GM, Lucas RM, Curran PJ, Honzak M. 1997. Non-linear mixture modelling without end-members using an artificial neural network. *International Journal of Remote Sensing* **18**: 937-953.

Foppa N, Wunderle S, Hauser A, Oesch D, Kuchen F. 2004. Operational sub-pixel snow mapping over the Alps with NOAA AVHRR data. *Annals of Glaciology* **38**: 245-252.

Global Land Cover Facility. 2009. Earth Science Data Interface (ESDI). Available online at http://glcf.umiacs.umd.edu/index.shtml. [last accessed on August 11, 2009]

Hall DK, Foster JL, Salomonson VV, Klein AG, Chien JYL. 2001. Development of a technique to assess snow-cover mapping errors from space. *IEEE Transactions on Geoscience and Remote Sensing* **39**: 432-438.

Hall DK, Riggs GA, and Salomonson VV. 1995. Development of methods for mapping global snow cover using moderate resolution imaging spectroradiometer data. *Remote Sensing of Environment* **54**: 127-140.

Hall DK, Riggs GA, Salomonson VV, DiGirolamo NE, Bayr KJ. 2002. MODIS snow-cover products. *Remote Sensing of Environment* **83**: 181-194.

Haykin S. 1999. *Neural Networks: A Comprehensive Foundation.* Prentice Hall: Upper Saddle River; 842.

Hodges J. 2002. *MODIS MOD12 Land Cover and Land Cover Dynamics Products User Guide*. Available online at http://www-modis.bu.edu/landcover/userguidelc/. [last accessed on August 16, 2009]

Hongen, Z., and L. Suhong. 2004. Moderate fraction snow mapping in Tibetan Plateau. *Proceedings of IGARSS'04* **6**: 3700-3701. DOI: 10.1109/IGARSS.2004.1369923.
Jensen JR. 2005. *Introductory Digital Image Processing: A Remote Sensing Perspective*. Clarke KC (ed). Pearson Prentice Hall: Upper Saddle River
Kaufmann YJ, Wald AE, Remer LA, Gao B, Li R, Flynn L. 1997. The MODIS 2.1-mm channel-correlation with visible reflectance for use in remote sensing of aerosol. *IEEE Transactions on Geoscience and Remote Sensing* **35**: 1286-1298.
Klein AG, Hall DK, Riggs GA. 1998. Improving snow cover mapping in forests through the use of a canopy reflectance model. *Hydrological Processes* **12**: 1723-1744.
König M, Winther J, Isaksson E. 2001. Measuring snow and glacier ice properties from satellite. *Reviews of Geophysics* **39**: 1-27.
Lee S, Lathrop RG. 2006. Subpixel analysis of Landsat ETM+ using Self-Organizing Map (SOM) neural networks for urban land cover characterization. *IEEE Transactions on Geoscience and Remote Sensing* **44**: 1642-1654. DOI: 10.1109/TGRS.2006.869984.
Lemke P, Ren J, Alley RB, Allison I, Carrasco J, Flato G, Fujii Y, Kaser G, Mote P, Thomas RH, Zhang T. 2007. Observations: Changes in Snow, Ice and Frozen Ground. In *Climate Change 2007: The Physical Science Basis. Contribution of Working Group I to the Fourth Assessment Report of the Intergovernmental Panel on Climate Change*, Solomon S, Qin D, Manning M, Chen Z, Marquis M, Averyt KB, Tignor M, Miller HL (eds). Cambridge University Press: Cambridge, New York; 337-383.
Metsämäki SJ, Anttila ST, Markus HJ, Vepsalainen JM. 2005. A feasible method for fractional snow cover mapping in boreal zone based on a reflectance model. *Remote Sensing of Environment* **95**: 77-95.
National Aeronautics and Space Administration. 2009. *Landsat 7 Science Data Users Handbook 2009*Available online at http://landsathandbook.gsfc.nasa.gov/handbook.html. [last accessed on August 11, 2009.
Niu GY, Yang ZL. 2007. An observation-based formulation of snow cover fraction and its evaluation over large North American river basins. *Journal of Geophysical Research-Atmospheres* **112**. DOI: 10.1029/2007JD008674
Nolin AW, Dozier J. 1993. Estimating snow grain-size using AVIRIS data. *Remote Sensing of Environment* **44**: 231-238.
Painter TH, Dozier J, Roberts DA, Davis RE, Green RO. 2003. Retrieval of subpixel snow-covered area and grain size from imaging spectrometer data. *Remote Sensing of Environment* **85**: 64-77.
Painter TH, Rittger K, McKenzie C, Slaughter P, Davis RE, Dozier J. 2009. Retrieval of subpixel snow covered area, grain size, and albedo from MODIS. *Remote Sensing of Environment* **113**: 868-879.
Priddy KL, Keller PE. 2005. *Artificial Neural Networks: An Introduction (SPIE Tutorial Texts in Optical Engineering, Vol. TT68).* SPIE Publications: Bellingham; 180.
Rango, A. 1996. Spaceborne remote sensing for snow hydrology application. *Hydrological Sciences* **41**: 477-494.
Riggs GA, Hall DK, Salomonson VV. 2006. *MODIS Snow Products User Guide to Collection 5 2006*. Available online at http://modis-snow-ice.gsfc.nasa.gov/sug_c5.pdf. [last accessed on August 16, 2009]
Roesch A, Wild M, Gilgen H, Ohmura A. 2001. A new snow cover fraction parametrization for the ECHAM4 GCM. *Climate Dynamics* **17**: 933-946.
Romanov P, Tarpley D, Gutman G, Carroll T. 2003. Mapping and monitoring of the snow cover fraction over North America. *Journal of Geophysical Research-Atmospheres* **108**. DOI: 10.1029/2002JD003142
Salomonson VV, Appel I. 2004. Estimating fractional snow cover from MODIS using the normalized difference snow index. *Remote Sensing of Environment* **89**: 351-360.
Salomonson VV, Appel I. 2006. Development of the Aqua MODIS NDSI fractional snow cover algorithm and validation results. *IEEE Transactions on Geoscience and Remote Sensing* **44**: 1747-1756.
Schowengerdt RA. 1997. *Remote Sensing: Models and Methods for Image Processing*. Academic Press: San Diego; 522.

Shabanov, N. V., K. Lo, S. Gopal, and R. B. Myneni. 2005. Subpixel burn detection in Moderate Resolution Imaging Spectroradiometer 500-m data with ARTMAP neural networks. *Journal of Geophysical Research-Atmospheres* **110**. DOI: 10.1029/2004JD005257.

Shi J. 1999. Estimation of snow fraction using AVIRIS simulated ASTER image data. Proceedings of IGARSS'99 3: 1795-1797. DOI: 10.1109/IGARSS.1999.772098.

Simpson JJ, McIntire TJ. 2001. A recurrent neural network classifier for improved retrievals of areal extent of snow cover. IEEE *Transactions on Geoscience and Remote Sensing* **39**: 2135-2147.

Simpson JJ, Stitt JR, Sienko M. 1998. Improved estimates of the areal extent of snow cover from AVHRR data. *Journal of Hydrology* **204**: 1-23.

Tatem AJ, Lewis HG, Atkinson PM, Nixon MS. 2002. Super-resolution land cover pattern prediction using a Hopfield neural network. *Remote Sensing of Environment* **79**: 1-14.

Vermonte EF, Kotchenova SY. 2008. MOD09 (Surface Reflectance) User's Guide. Available online at http://modis-sr.ltdri.org/MAIN_SURFACE_PRODUCTAND%20USER%20GUIDE/MOD09_UserGuide.pdf [last accessed on August 16, 2009]

Vikhamar D, Solberg R. 2002. Subpixel mapping of snow cover in forests by optical remote sensing. *Remote Sensing of Environment* **84**: 69-82.

Vikhamar D, Solberg R. 2003. Snow-cover mapping in forests by constrained linear spectral unmixing of MODIS data. *Remote Sensing of Environment* **88**: 309-323.

Wolfe RE. 2006. *MODIS Geolocation. In Earth Science Satellite Remote Sensing.* Springer: Berlin, New York; 50-73.